High temperature breakdown of the Stokes-Einstein relation in a computer simulated Cu-Zr melt

X. J. Han, , J. G. Li, and , and H. R. Schober

Citation: The Journal of Chemical Physics **144**, 124505 (2016); doi: 10.1063/1.4944081
View online: http://dx.doi.org/10.1063/1.4944081
View Table of Contents: http://aip.scitation.org/toc/jcp/144/12
Published by the American Institute of Physics

High temperature breakdown of the Stokes-Einstein relation in a computer simulated Cu-Zr melt

X. J. Han,[1,a)] J. G. Li,[1,b)] and H. R. Schober[2,c)]
[1]*School of Materials Science and Engineering, Shanghai Jiao Tong University, Dongchuan Rd. 800, 200240 Shanghai, People's Republic of China*
[2]*Peter Grünberg Institut, Forschungszentrum Jülich, D-52425 Jülich, Germany*

(Received 16 September 2015; accepted 2 March 2016; published online 23 March 2016)

Transport properties and the Stokes-Einstein (SE) relation in liquid Cu_8Zr_3 are studied by molecular dynamics simulation with a modified embedded atom potential. The critical temperature T_c of mode coupling theory (MCT) is derived as 930 K from the self-diffusion coefficient D and viscosity η. The SE relation breaks down around T_{SE} = 1900 K, which is far above T_c. At temperatures below T_{SE}, the product of D and η fluctuates around a constant value, similar to the prediction of MCT near T_c. The influence of the microscopic atomic motion on macroscopic properties is investigated by analyzing the time dependent liquid structure and the self-hole filling process. The self-holes for the two components are preferentially filled by atoms of the same component. The self-hole filling dynamics explains the different breakdown behaviors of the SE relation in Zr-rich liquid $CuZr_2$ compared to Cu-rich Cu_8Zr_3. At T_{SE}, a kink is found in the temperature dependence of both partial and total coordination numbers for the three atomic pair combinations and of the typical time of self-hole filling. This indicates a strong correlation between liquid structure, atomic dynamics, and the breakdown of SE relation. The previously suggested usefulness of the parameter $d(D_1/D_2)/dT$ to predict T_{SE} is confirmed. Additionally we propose a viscosity criterion to predict T_{SE} in the absence of diffusion data. © *2016 AIP Publishing LLC.* [http://dx.doi.org/10.1063/1.4944081]

I. INTRODUCTION

By combining Einstein's theory of the diffusion of small suspended particles[1] and Stokes' law for the drag of a mesoscopic ball in a viscous fluid,[2] the well-known Stokes-Einstein (SE) relation[3,4] is derived as

$$D = k_bT/(cd\eta), \quad (1)$$

where D is the diffusion coefficient, η the shear viscosity of the liquid, d the particle diameter, k_b the Boltzmann constant, T the temperature, and c is a constant depending on the boundary condition at the particle/fluid interface. For slip and stick interfacial boundary conditions, c is 2π and 3π, respectively. The slip boundary condition seems to be the most appropriate when the interaction between solvent and solute particles is a central force with no tangential component,[5] and it has been widely applied in theoretical analysis[6] and in molecular dynamics (MD) studies.[7–10] Following these studies, we use slip boundary conditions in this work. In undercooled glass forming melts, the viscosity determines the decay time of the α-relaxation. Therefore, especially in theoretical work, the SE relation is often written in terms of the α-relaxation time, τ_α, instead of the viscosity.[11–14] The SE relation was derived for a mesoscopic ball suspended in a continuum fluid; however, many experiments have demonstrated that in many liquids, Eq. (1) holds at a microscopic level over a large temperature range for the self-diffusion coefficient.[15–17]

On time scales beyond the vibrational regime, the two key dynamical properties, D and η, largely determine the dynamics of liquids. The SE relation is, therefore, of great significance in the studies of dynamics related phenomena such as nucleation, crystal growth, and the liquid-to-glass transition. For example, the decoupling of crystal growth kinetics from viscous flow near the glass transition temperature is due to the breakdown of SE relation, namely, the decoupling of D from η.[18–20] The violation of the SE relation upon cooling of a glass-forming liquid is also very important to understand the dramatic slowing down of the dynamics, accompanying the formation of a glass.[21,22] In the past several decades, the SE relation, especially its breakdown, has attracted considerable research interest of scientists in many fields.[7–17,23–29]

There are three unsolved, open questions regarding the breakdown of SE relation, namely, how far can one cool down the liquid before the SE relation breaks down, what mechanism is responsible for the breakdown, and how does one predict the onset of the breakdown quantitatively. The answers to these three interrelated questions are still discussed controversially.

Generally, at very high temperatures (HTs), above the liquidus temperature T_L, the SE relation describes the correlation between D and η reasonably well. In the absence of accurate measurements of the two parameters, it is often assumed[24–29] that the SE relation breaks down when the liquid is undercooled to temperatures near the critical temperature, T_c, of the mode coupling theory (MCT),[30] that is one of the most successful theories describing the dynamics of undercooled liquids. This assumption is consistent with the prediction of MCT that the atomic motion switches from the ergodic

a)E-mail: xjhan@sjtu.edu.cn. URL: http://orcid.org/0000-0003-3353-4183.
b)E-mail: lijg@sjtu.edu.cn
c)E-mail: h.schober@fz-juelich.de

liquid-like viscous flow to non-ergodic solid-like hopping when the liquid is quenched to T_c. However, many recent studies on glass-forming liquids, such as Zr-Ti-Cu-Ni-Be,[31] Ni-Zr-Al,[9] Ni-Zr,[32] Cu-Zr,[10] and Cu-Zr-Al,[33] have shown that the SE relation already breaks down at temperatures far above T_c, and even above T_L. Using electrostatic levitation technique, Brillo *et al.*[32] measured both η and D_{Ni} in liquid $Zr_{64}Ni_{36}$ over a temperature range of 800 K and found

$$D_{Ni}(T) \cdot \eta(T) \approx const., \tag{2}$$

in striking contrast to $D_{Ni}(T) \cdot \eta(T) \propto T$, as predicted by the SE relation. Expression (2) is seen in MCT near T_c, but this cannot explain why it still holds 500 K above T_L. Therefore, the abnormal breakdown of SE relation at temperatures far above T_c is a real challenge to experiment and theory.[34] Until now, experimental and MD studies of the abnormal breakdown of the SE relation mainly focused on Zr-based glass-forming liquids. It is still unclear whether it also occurs in a non-Zr-based liquid. This motivated us in this work to go one step further and check the SE relation of a Cu-based liquid Cu_8Zr_3 by MD simulation.

The breakdown of the SE relation in highly undercooled liquids close to T_c is often explained by a change of the mechanism of atomic motion,[28] dynamical heterogeneity,[11,16,27,35–39] or the coupling model by Ngai.[40,41] However, these explanations could not be applied directly to the abnormal breakdown of the SE relation at temperatures far above T_c, and even above T_L. In our previous MD study of liquid $CuZr_2$,[10] we found that the SE relation breaks down abnormally about 200 K above T_L. According to the temperature dependences of the ratio of the diffusivities of the two components, $d(D_1/D_2)/dT$, and the non-Gaussian parameter, the abnormal breakdown of SE relation is ascribed to a sudden increase of dynamical heterogeneity. Meanwhile, we demonstrated that the dynamical difference for the two components has an obvious effect on the macroscopic properties, as well as the breakdown of the SE relation. In liquid $CuZr_2$, the "self-hole" left by one Cu atom after it moves away is preferentially filled by another Cu atom, whereas for Zr this preferential self-hole filling by atoms of the same type does not take place.[42] The quite different self-hole filling dynamics for the two components leads to the earlier deviation from the SE relation for Cu than for Zr. We concluded in our work of $CuZr_2$ that the dynamical difference for the two components is a composition dependent phenomenon, and it might disappear in a Cu-based liquid. Therefore, investigations on the microscopic dynamics of liquid Cu_8Zr_3 will shed further light on the dynamical origin of the abnormal breakdown of the SE relation.

Formerly,[10] we proposed that in a binary system the ratio of the two self-diffusivities, D_1/D_2, could be used for predicting the breakdown temperature of the SE relation, T_{SE}. And using a Lennard-Jones liquid, we have already validated the universality of D_1/D_2 criterion for binary system. In this work, we would check the reasonability of this criterion in a Cu-based binary liquid. Moreover, we will go a step further to explore some other alternatives to predict T_{SE} in the absence of diffusion data.

The organization of the rest of the paper is as follows. In Sec. II, we describe the system studied and the applied simulation methods. The results of the simulation are given in Sec. III. Self-diffusion coefficient and viscosity are calculated, and T_c is derived from their temperature dependences. Based on the simulated data, the breakdown of the Stokes-Einstein relation is reported. Starting from the van Hove correlation function, the time dependent pair distribution function (PDF), the filling process of self-hole, and dynamic heterogeneity are studied. New criteria are given for the prediction of T_{SE}. In Sec. IV, the results are discussed in the context of our previous work and works of other groups. We end with a summary in Sec. V.

II. SIMULATION DETAILS

The molecular dynamics simulations are performed for systems of $N = 1188$ atoms with periodic boundary conditions in all three directions. The velocity Verlet algorithm with a time step of 2.5 fs is used to solve the equations of motion. Zero pressure was kept using the Parrinello-Rahman algorithm[43] with a volume mass of $\sqrt{N}m_{Zr}$, where N is the number of particles and m_{Zr} the atomic mass of Zr. To prevent oscillations, an additional damping term was used. The temperature was controlled by a Nóse-thermostat, following Hoover.[44] The atomic interaction is modeled by a modified embedded atom method (MEAM).[45] Details of the potential for the Cu-Zr binary system were given in our previous works.[10,46,47]

Liquid Cu_8Zr_3 is first equilibrated at 2500 K for 2 nanoseconds (ns). For the subsequent calculations, after equilibration, configurations were saved every 2 ns. In total, we use four independent samples to improve the statistics. Each sample is quenched to 1300 K in steps of 100 K with a cooling rate of 10^{12} K/s. At each considered temperature before evaluating, the quantities presented below, the samples are additionally equilibrated for 2.5 ns, much longer than the typical relaxation time of the system. The evaluation times range from 5 ns to 15 ns, depending on the temperature. Within the temperature range investigated in this work, no aging effects are observed during the evaluation.

A. Calculation of the self-diffusion coefficients and viscosity

The self-diffusion coefficients for the two species are calculated from the long time evolution of their respective mean-square displacements (MSDs),[48]

$$\langle r^2(t) \rangle = \frac{1}{N} \sum_{i=1}^{N} [r_i(t) - r_i(0)]^2, \tag{3}$$

by the standard expression

$$D = \lim_{t \to \infty} \frac{1}{6t} \langle r^2(t) \rangle, \tag{4}$$

where $\langle \ldots \rangle$ denotes the ensemble average and the sum is over all atoms of Cu and Zr, respectively.

According to the Green-Kubo equation,[48,49] the shear viscosity η is expressed by the time integral over the stress

auto-correlation function $\tilde{\eta}(t)$,

$$\eta = \int_0^\infty \tilde{\eta}(t)dt, \tag{5}$$

$$\tilde{\eta}(t) = \frac{1}{k_B T V} \langle \sigma^{xy}(t) \cdot \sigma^{xy}(0) \rangle , \tag{6}$$

where V is the volume of the system, T the temperature, k_B the Boltzmann constant, and σ^{xy} stands for the off-diagonal elements of the macroscopic stress tensor computed from the momenta and virials,

$$\sigma^{kl} = \sum_i \left(m_i v_i^k v_i^l - \sum_{j>i} \frac{\partial U}{\partial r_{ij}} \frac{r_{ij}^k r_{ij}^l}{r_{ij}} \right) \quad k,l = x,y,z. \tag{7}$$

Here $\boldsymbol{r_i}$ and $\boldsymbol{v_i}$ are the coordinates and velocities, respectively, of particle i, $\boldsymbol{r_{ij}}$ is the vector connecting particles i and j, m_i is the mass of particle i, U is the potential energy of the system, and $\boldsymbol{F}_{ij} = -\partial U/\partial \boldsymbol{r}_{ij}$ is the force exerted by particle j onto particle i. More details of the adopted procedure can be found in our previous work.[10]

B. Calculation of the pair correlations

The pair correlations are described by the distinct parts of the van Hove correlation functions,[42]

$$G_{\alpha\beta}^d(\mathbf{r},t) = \frac{V}{N_\alpha (N_\alpha - 1)} \sum_{\substack{i,j=1 \\ i\neq j}}^{N_\alpha} \delta \left(\mathbf{r} - \left(\mathbf{R}_\alpha^j(t) - \mathbf{R}_\alpha^i(0) \right) \right)$$

$$\text{for } \alpha = \beta, \tag{8}$$

$$G_{\alpha\beta}^d(\mathbf{r},t) = \frac{V}{N_\alpha N_\beta} \sum_{i=1}^{N_\alpha} \sum_{j=1}^{N_\beta} \delta \left(\mathbf{r} - \left(\mathbf{R}_\beta^j(t) - \mathbf{R}_\alpha^i(0) \right) \right)$$

$$\text{for } \alpha \neq \beta. \tag{9}$$

Here α and β denote the atomic species, V the volume, N_α the number of atoms of species α, and $\mathbf{R}$ gives the atomic position.

The time dependent radial pair distribution function is defined as the orientational average of $G_{\alpha\beta}^d(\mathbf{r},t)$,

$$g_{\alpha\beta}(r,t) = \frac{1}{4\pi r^2} \int G_{\alpha\beta}^d(\mathbf{r},t)\, d\Omega. \tag{10}$$

III. SIMULATION RESULTS

A. Diffusion coefficients

The self-diffusion coefficients for the two species are evaluated from the slopes of the MSDs in the long range diffusive regime, namely, for $t > 5$ ps, according to Eq. (4). The results are illustrated in a semi-logarithmic plot in Fig. 1, where the solid squares (■) and solid circles (●) represent the diffusion data for Cu and Zr in liquid Cu_8Zr_3, respectively. Following MCT,[30] the self-diffusion coefficients for not too high temperatures can be described by a power function of the critical temperature T_c,

$$D(T) = D_0^{MCT}(T - T_c)^\gamma. \tag{11}$$

Data regression indicates that in the temperature regime (1300 K and 2000 K), the two coefficients can be fitted by the MCT expression with a common T_c of 930 K, and γ-values of 1.25 and 2.11 for Cu and Zr, respectively. In our previous work on liquid $CuZr_2$, we found T_c = 1025 K and γ values of 1.52 and 1.93 for Cu and Zr, respectively. Compared with liquid $CuZr_2$, Cu_8Zr_3 has a lower T_c and a larger difference between the two γ-values. The diffusion data in the investigated temperature range can also be fitted by an Arrhenius law,

$$D = D_0 \exp(-Q/RT), \tag{12}$$

where Q is the activation energy, and R the gas constant, 8.314 J/mol · K. For Cu and Zr, we find $D_0 = 5.9 \times 10^{-8}$ and 1.1×10^{-7} m^2/s, and Q = 41 489 and 64 399 J/mol, respectively. In this particular substance over the investigated temperature range, the deviation of the diffusion coefficient from the Arrhenius law is very small. A larger effect is seen in the viscosity, further down.

For comparison, we include in Fig. 1 also the diffusion data of liquid $CuZr_2$, shown by open diamonds (◊) and open upper triangles (△). The diffusivity of Zr varies only weakly with composition. In contrast, Cu has, for the higher concentration, a markedly enhanced diffusivity and a more pronounced temperature dependence. The diffusion coefficients for the two species in liquid Cu_8Zr_3 do not run parallel to each other as a function of temperature. This is similar to the case of liquid $CuZr_2$; however, the effect is reduced. The self-diffusion coefficients for Zr in the two compositions are quite close to each other at temperatures above 1600 K, whereas Cu diffuses much faster in liquid Cu_8Zr_3 than it does in liquid $CuZr_2$. Recently, D_{Cu} in liquid $CuZr_2$ was measured experimentally by Yang *et al.*[50] using a combination of containerless processing technique and quasielastic neutron scattering, shown by open squares (□) in Fig. 1. The simulated liquidus temperature of $CuZr_2$, T_m^{MD}, is 1478.5 K according to our previous MD work,[10] and the experimental value, T_m^{Exp}, is 1315 K. These two liquidus temperatures should be treated as equivalent regardless of the difference of around 11%. D_{Cu} in our MD simulation at T_m^{MD} is around 1.09×10^{-9} m^2/s, denoted by the open circle (○), which agrees well with the experimental value of $(1.19 \pm 0.11) \times 10^{-9}$ m^2/s at T_m^{Exp}, the deviation being less than 9%.

Due to the lack of experimental data for liquid Cu_8Zr_3, it is difficult to give a direct comparison of our simulation work with experimental studies. Mendelev *et al.* studied the self-diffusivities of liquid $Cu_{70}Zr_{30}$ using MD with an EAM potential, the so-called MKOSYP.[51] For comparison, we show the predicted D_{Cu} (⊕) and D_{Zr} (▽) at 1500 and 1200 K. Clearly, at 1500 K D_{Cu} from MKOSYP agrees quite well with the one in this work, whereas at 1200 K the former (4.35×10^{-10} m^2/s) is much lower than the latter (~8.0×10^{-10} m^2/s). Our D_{Zr} at 1500 K, 6.54×10^{-10} m^2/s, is much lower than that from MKOSYP, 1.53×10^{-9} m^2/s, but at 1200 K, our extrapolated value of 1.5×10^{-10} is close to Mendelev's 2.3×10^{-10} m^2/s. For the Cu-Zr system, Mendelev *et al.* presented another EAM, the so-called MSK,[52] parameterized using force matching method. Both MKOSYP and MSK predict the structure well; however, the predictions

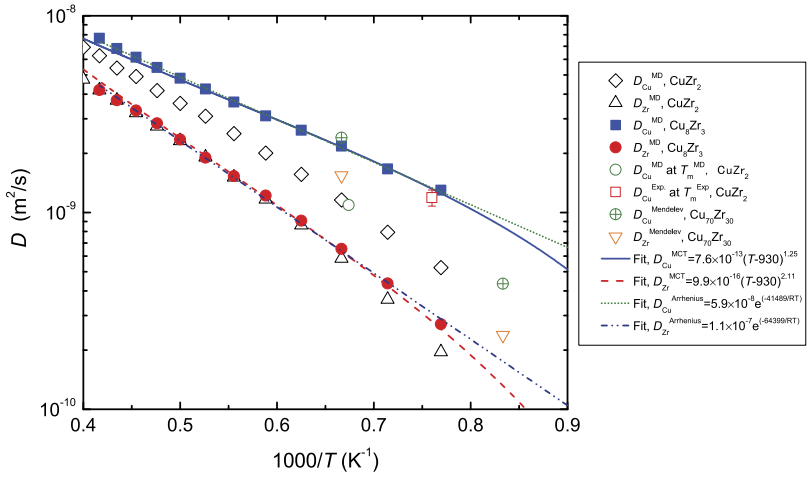

FIG. 1. Self-diffusion coefficients of Cu and Zr in liquid Cu_8Zr_3 and $CuZr_2$ against temperature.

of the self-diffusivities are quite different. For example, for liquid $Cu_{64}Zr_{36}$, at 1500 K, D_{Cu} ranges from 2.1×10^{-9} (MSK) to 3.4×10^{-9} (MKOSYP), and D_{Zr} differs from 1.5×10^{-9} (MSK) to 2.6×10^{-9} (MKOSYP) m^2/s. This uncertainty becomes larger with decreasing temperature. At 1200 K, the results from MKOSYP are even 3–4 times of that of MSK. Considering the uncertainties of the models of Mendelev *et al.* in predicting diffusivities, the results in this work should be within the range of their predictions.

To elucidate the divergence of the two diffusivities, we report in Fig. 2 the ratio between the two coefficients, D_{Cu}/D_{Zr}, for liquid Cu_8Zr_3 and $CuZr_2$. Clearly, there are two temperature regimes separated by T_s. At temperatures above T_s, D_{Cu}/D_{Zr} increases only slightly with temperature. However, when the liquid is cooled to below T_s, the ratio D_{Cu}/D_{Zr} increases rather rapidly as the temperature decreases. T_s is 1900 and 1600 K for Cu_8Zr_3 and $CuZr_2$, respectively. Taking into account that Cu and Zr share a common critical temperature T_c, a divergence of D_{Cu}/D_{Zr} upon approaching T_c results from the different $\gamma-$values of the two components, see Eq. (11). The difference

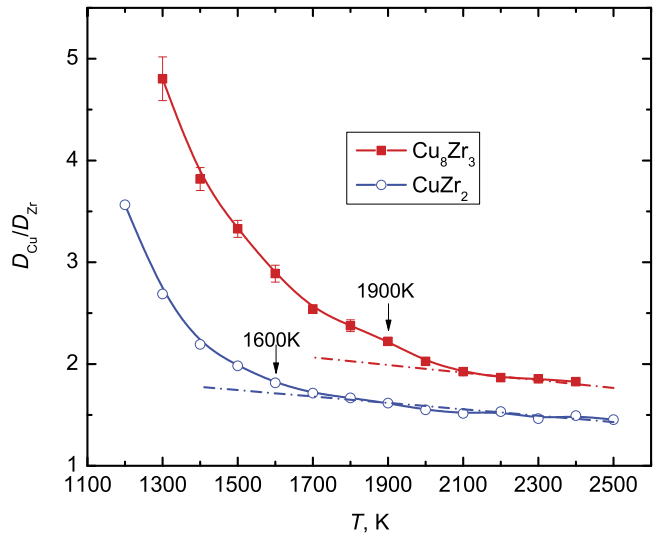

FIG. 2. Averaged ratio of the diffusion coefficients, D_{Cu}/D_{Zr}, in liquid Cu_8Zr_3 and $CuZr_2$ versus temperature. The arrows indicate the crossover temperature T_s. The dashed-dotted lines show the extrapolation from high temperatures.

in the T_s values between the two compositions is much larger than expected from the corresponding difference of the T_c values, indicating a difference in the atomic dynamics.

B. Calculation of the viscosity

The viscosities of liquid Cu_8Zr_3 at different temperatures are evaluated from the integral of the stress autocorrelation functions according to Eqs. (5)-(7), and the results are reported in Fig. 3. An Arrhenius relation $\eta = \eta_0 \exp(Q/RT)$ describes the temperature dependence of the viscosity only for temperatures above 2000 K. Data regression gives a prefactor $\eta_0 = 0.48$ mPa s and an activation energy of 38 032 J/mol, somewhat less than the diffusional activation energy. The viscosity data at temperatures below 2000 K can again be fitted by an MCT formula

$$\eta = \eta_0 (T - T_c)^{-\gamma}, \tag{13}$$

with $T_c = 930$ K, as for diffusion, and $\gamma = 1.87$, which lies between the diffusional values for the two components.

For comparison, in Fig. 3, we also show the viscosity data of liquid $CuZr_2$. For both compositions, the switch from the Arrhenius dependence at high temperatures to the MCT one occurs near T_s, as determined from the ratio of the diffusivities. Such break away of the shear viscosity from its Arrhenius behavior at high temperatures can also be found in other systems, for example, in a model Lennard-Jones liquid[53] and in regular liquid metals.[54] This switch of the temperature behavior of viscosity hints at a variation of dynamics in the liquid. Noticeably, T_s of liquid $CuZr_2$ has been found to correspond to the breakdown temperature of the SE relation for the self-diffusion of Zr and the effective mean diffusion. The correlations of T_s and the breakdown temperature of SE relation in liquid Cu_8Zr_3 are discussed in Sec. III C. If the SE relation in this work also breaks down at T_s, we might assume that this phenomenon is not an accident, and the deviation of the viscosity from the Arrhenius behavior could be applied to quantitatively predict the onset of the breakdown of the SE relation. Thus, besides the ratio of the two self-diffusivities, D_{Cu}/D_{Zr}, we will have another criterion from the viscosity side, which will not be limited to a binary system. This would be quite useful for experimentalists when using the SE

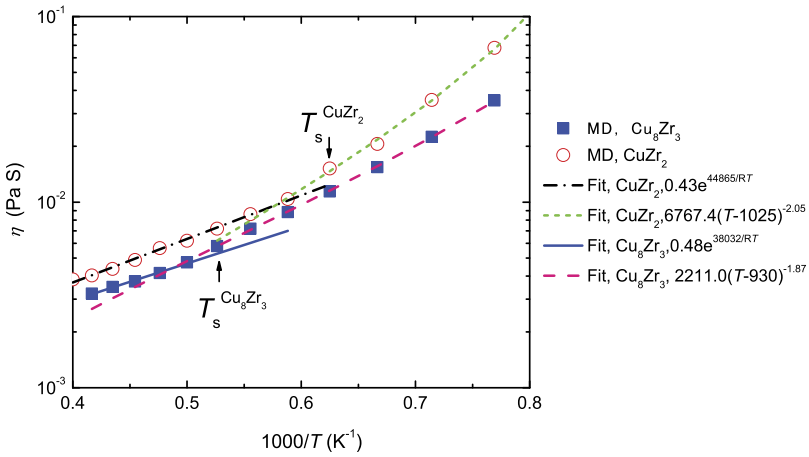

FIG. 3. Viscosities of liquid Cu_8Zr_3 and $CuZr_2$ against temperature. The lines show the high temperature Arrhenius fits and the low temperature (LT) MCT fits. The arrows indicate T_s as estimated from the ratio of the diffusion coefficients, Fig. 2.

relation in the absence of either viscosity or diffusion data. The physical picture behind T_s will be clarified further down.

C. Breakdown of Stokes-Einstein relation

In the original SE relation, Eq. (1), the effective diameter d_{SE} is a constant. A possible temperature dependence of the effective atomic diameter is weak. For the convenience of evaluating the breakdown of the SE relation, we treat the effective diameter as a function of temperature

$$d_{SE}(T)=\frac{k_B T}{2\pi\eta(T)D(T)}. \tag{14}$$

Therefore, as long as $d_{SE}(T)$ is a constant, independent of temperature, the SE relation is deemed to hold, otherwise, the SE relation has broken down.

The calculated viscosity and diffusion coefficients, d_{SE} at different temperatures are illustrated in Fig. 4, where solid symbols represent d_{SE} for D_{Zr}, and the open ones d_{SE} for D_{Cu}. Apparently, for the two species at temperatures above 2000 K, d_{SE} fluctuates around values, $d_0 \approx 3.90$ Å and $d_0 \approx 2.05$ Å, for Zr and Cu, respectively. However, the two $d_{SE}(T)$ values start to deviate from their respective d_0 at a temperature of about

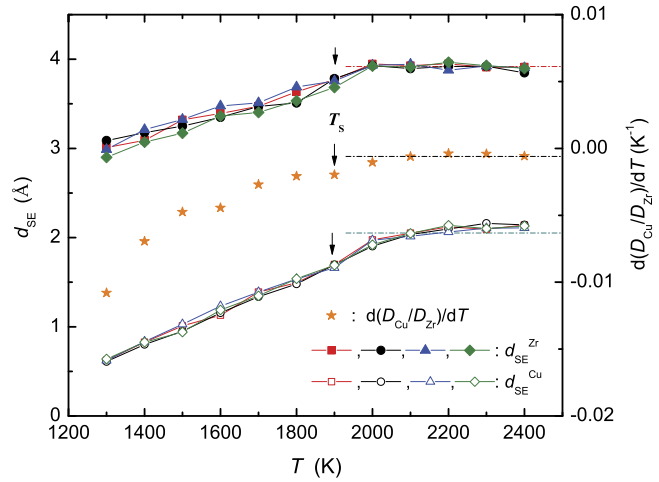

FIG. 4. Effective SE diameters $d_{SE}(T)$ for four independent samples, indicated by different symbols, Zr top and Cu bottom. The derivative $d(D_{Cu}/D_{Zr})/dT$ is indicated by asterisks. The dashed-dotted lines show the high temperature asymptotic values.

2000 K. This means that the SE relation breaks down at a temperature between 1900 K and 2000 K, near T_s. Considering T_c (~930 K) derived from D and η in Secs. III A and III B, the SE relation breaks down in liquid Cu_8Zr_3 already at a temperature twice the MCT T_c, similar to the earlier findings in liquid $CuZr_2$.

In our previous work on $CuZr_2$, we related the abovementioned d_0 to the nearest neighbor distance d_1, since d_0^{Zr} agrees quite well with d_1^{Zr}. However, in the same liquid and with the same slip boundary condition, d_0^{Cu} is 16% less than d_1^{Cu}. The difference between d_0 and d_1 is even more pronounced in liquid Cu_8Zr_3, because the d_0^{Cu} values in both liquids are almost identical, whereas d_0^{Zr} in liquid Cu_8Zr_3 is more than 25% higher than in liquid $CuZr_2$. This indicates that it is difficult to directly relate d_0 to d_1, and the atomic dynamics influences the value of d_0. This might be caused by a change of the atomic boundary condition in the SE-relation (slip to stick) or, probably, by a more complicated effect due to the increasing collectivity of motion.

Included in Fig. 4 is also the temperature derivative of the ratio of the two self-diffusivities, $d(D_{Cu}/D_{Zr})/dT$, denoted by asterisks. At temperatures above 2000 K, $d(D_{Cu}/D_{Zr})/dT$ fluctuates around -6×10^{-4} K^{-1}, which indicates that D_{Cu}/D_{Zr} increases linearly and slightly as the temperature decreases. Below 2000 K, the slope changes abruptly and $d(D_{Cu}/D_{Zr})/dT$ deviates strongly from the constant value, indicating that D_{Cu}/D_{Zr} increases more and more rapidly with the further decrease of the temperature. This observation supports the conclusion in our previous work that in a binary system $d(D_{Cu}/D_{Zr})/dT$ correlates closely with the effective diameter d_{SE} and can be used to predict the onset of the breakdown of the SE relation.

We show the product of self-diffusion coefficient and viscosity, $D\cdot\eta$, of liquid Cu_8Zr_3 in Fig. 5, for D_{Cu}, D_{Zr}, and $D_{eff} = (\sum_i c_i/D_i)^{-1}$, which is an approximate description of diffusion for a multi-component system in terms of an effective monatomic one. For comparison, we include the $D\cdot\eta$ values of liquid $CuZr_2$ as open squares, circles, and diamonds for D_{Cu}, D_{Zr}, and D_{eff}, respectively. At temperatures above T_{SE} (2000 K and 1700 K for liquid Cu_8Zr_3 and $CuZr_2$, respectively), both $D_{Cu}\cdot\eta$ and $D_{Zr}\cdot\eta$ change linearly with temperature, consistent with the SE relation in this temperature regime. In this high temperature regime, $T > T_{SE}$, both the values of $D_{Cu}\cdot\eta$ and

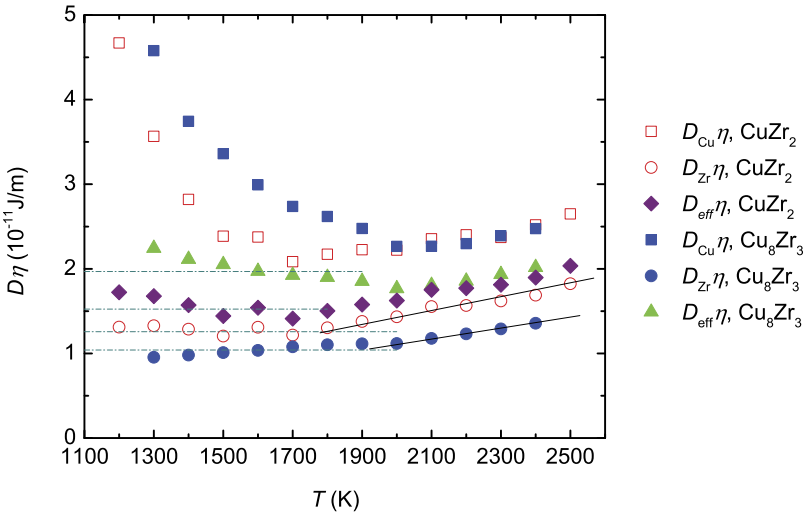

FIG. 5. Products of D and η in liquid Cu_8Zr_3 and $CuZr_2$ at different temperatures. The lines are guides to the eye to indicate the crossover between the high and low temperature regimes.

$D_{\text{eff}}\cdot\eta$ for the two compositions are similar whereas the $D_{\text{Zr}}\cdot\eta$ values strongly change with concentration. In contrast, at temperatures below T_{SE}, the temperature dependences of the three $D\cdot\eta$ vary and all values show a composition dependence. On one hand, with decreasing temperature, $D_{\text{Cu}}\cdot\eta$ increases rapidly. For both compositions $D_{\text{Cu}}\cdot\eta$ at the respective lowest temperature shown is around twice the value at the respective T_{SE}. On the other hand, at these temperatures below T_{SE}, $D_{\text{Zr}}\cdot\eta$ levels off at values around 1.26 and 1.03 for liquid $CuZr_2$ and Cu_8Zr_3, respectively. For both compositions, $D_{\text{eff}}\cdot\eta$ shows a behavior similar to the one of Zr.

MCT predicts the same parameter γ for diffusion coefficient and viscosity (see Eqs. (11) and (12)), and thus the product of D and η should be a constant. In the earlier work on $CuZr_2$, we found $\gamma = 1.92$ from D_{Zr} and $\gamma = 2.05$ from viscosity. For Cu_8Zr_3 in this work, we get $\gamma = 2.11$ from D_{Zr}, and $\gamma = 1.87$ from the viscosity. The differences between the two γ-values are not too large, and the deviation is about 7% and 11% for $CuZr_2$ and Cu_8Zr_3, respectively. As a result, $D_{\text{Zr}}\cdot\eta$ in the two liquids does not change noticeably at temperatures below T_{SE}, where MCT describes both diffusion coefficient and viscosity quite well. Such behavior has also been observed in experiment. Measuring the self-diffusion coefficient and the viscosity of liquid $Zr_{64}Ni_{36}$ under electrostatic levitation, Brillo *et al.* observed $D\cdot\eta = const$ in a wide temperature range spanning 800 K.[27]

The diffusional MCT γ-values of Cu are in $CuZr_2$ 80% and in Cu_8Zr_3 only 60% of the respective ones derived from the viscosity, indicating a decoupling of the Cu diffusion from the effective medium responsible for viscosity. In our previous work on $CuZr_2$,[10] we found T_{SE} of copper 300 K higher than that of Zr. We ascribed this temperature difference to the qualitatively different dynamics of the two species. During diffusion on average, the site of a Zr atom is filled by another atom according to the concentration, and there is no preference toward the atom type. In contrast, a Cu atom is preferably replaced by another Cu atom. Such preferential replacement of a Cu atom by another Cu atom contributes to tracer diffusion but has little effect on viscosity, since the surroundings need not change. As a result, D_{Cu} and η in liquid $CuZr_2$ decouple already at a much higher temperature than D_{Zr}. Unlike this case of liquid $CuZr_2$, the SE relations in liquid Cu_8Zr_3 break down at similar temperatures for both Cu and Zr but $D\eta$ increases much more rapidly with decreasing temperature which would shift the break to higher temperatures. In our previous work on $CuZr_2$, we pointed out that the rather different dynamics of the two species is special and composition dependent, and it might disappear in Cu-rich liquid. In Sec. III D, we study the real space dynamics of the two species in liquid Cu_8Zr_3 and its possible correlation with the breakdown of SE relation.

D. Atomic dynamics

In Secs. III A–III C, we surmised that there is a close correlation between the microscopic dynamics of atomic motion and the macroscopic transport properties, as well as the breakdown of the SE relation. In this section, starting from the van-Hove correlation function, the time evolution of the liquid structure, the process of self-hole filling, and the dynamic heterogeneity in liquid Cu_8Zr_3 are studied to explore the microscopic details of atomic motion.

1. Static pair distribution function

The static total PDFs of liquid Cu_8Zr_3 are presented in Fig. 6. As examples, the results at 2400 and 1400 K are illustrated in Fig. 6(a). For comparison, the total PDFs calculated with LAMMPS[55] using the EAM models by Mendelev *et al.*[51] and Cheng *et al.*,[56] are included. The characteristic parameters for total PDFs from different sources are listed in Table I.

Generally, despite different parameterizations, these three potential models predict similar structures for liquid Cu_8Zr_3. The positions of the first peak, r_1, and first minimum, r_2, of the total PDFs for three models are mutually consistent at 2400 K. The differences are mainly in the radius of the self-hole, r_0, and the intensity of the first peak, $g(r_1)$. Our MEAM agrees quite well with Cheng's EAM in predicting r_0, which is about 8% larger than that from Mendelev's EAM. The first peak from our model is slightly broader and lower than those from the other two EAM models.

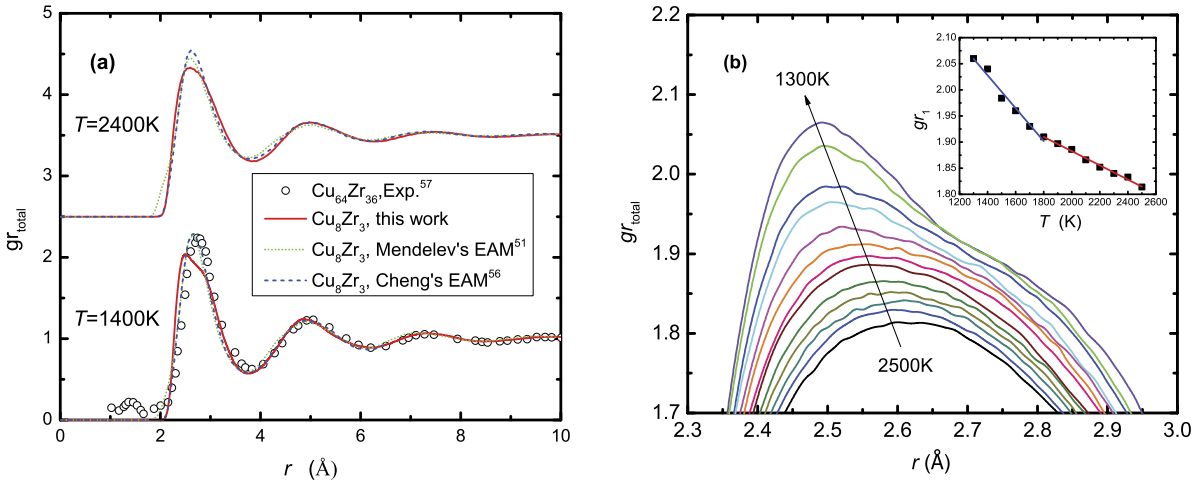

FIG. 6. Static total pair distribution functions of liquid Cu_8Zr_3. (a) Total PDFs from different sources. (b) Enlarged first peak of the total PDF at different temperatures. From bottom to top, the temperature decreases from 2500 to 1300 K in steps of 100 K. The inset illustrates the variation of the intensity of the first peak with temperature.

The coordination number (CN) is obtained by integrating the area under the first peak up to the first minimum

$$CN = \frac{N}{V}\int_0^{r_2} 4\pi r^2 g(r)dr, \tag{15}$$

where N is the total number of atoms and V the volume of the system. The number densities of the system (N/V) and the calculated CNs are also listed in Table I. Clearly, the number densities from three potentials are quite close to each other. The coordination number of 13.4 at 2400 K in this work is close to Mendelev's 13.0 and around 6% larger than Cheng's prediction. At 1400 K, our model gives an r_1 of 2.68 Å by averaging over the peak, which is consistent with the value of 2.65 Å from the other two models. The calculated CN in this work is close to predictions from Mendelev's and Cheng's models, and the deviations are about 3% and 6%, respectively. Due to the lack of experimental data, it is difficult to compare the simulation directly with experiment. Wessels *et al.* measured the structure of liquid $Cu_{64}Zr_{36}$ at 1400 K.[57] Assuming that there is no pronounced difference in the structure of liquid Cu_8Zr_3 and $Cu_{64}Zr_{36}$, the experimental data of liquid $Cu_{64}Zr_{36}$ are also included in Fig. 6(a) and compared with simulation results of liquid Cu_8Zr_3. It can be seen that the simulation in this work agrees well with the experimental results except for a slight shift of r_1 and an underestimate of $g(r_1)$. The variation of the first peak of the total PDF with the temperature is shown in Fig. 6(b). As usual, at high temperatures, the first peak is more or less symmetric. Interestingly, it becomes more and more asymmetric as the temperature decreases. The inset in Fig. 6(b) shows the change of $g(r_1)$ with temperature. As to be expected, the intensity shifts linearly with temperature. However, there is a clear change of slope at around 1800 K, quite close to T_s = 1900 K.

To gain some insight into the dependence of the PDFs on atomic species, the partial pair distribution functions (PPDFs) are illustrated in Fig. 7. As shown in Fig. 7(a), PPDFs at 2400 K, the positions of the first peaks are at 2.44, 2.84, and 2.97 Å for Cu-Cu, Cu-Zr, and Zr-Zr pairs, respectively. These distances vary little with temperature. Several authors have extracted PPDFs for CuZr glasses and melts. Blodgett and Kelton[58] find only a weak dependence of the positions of the first peaks of the PPDFs on concentration and temperature.

TABLE I. Values for the total PDF of liquid Cu_8Zr_3 from different sources. r_0: radius of the self-hole, r_1: position of the first peak, $g(r_1)$: intensity of the first peak, r_2: position of the first minimum, ρ: number density, CN: coordination number.

		This work	Mendelev's EAM[51]	Cheng's EAM[56]	Wessels's Expt.[57]
r_0 (Å)	2400 K	1.98	1.79	1.95	
	1400 K	2.04	1.85	2.03	1.8–2.00
r_1 (Å)	2400 K	2.60	2.60	2.64	
	1400 K	(2.68)[a]	2.65	2.65	2.72
$g(r_1)$	2400 K	1.83	1.95	2.05	
	1400 K	2.04	2.28	2.29	2.23
r_2 (Å)	2400 K	3.82	3.79	3.77	
	1400 K	3.78	3.75	3.75	3.83
ρ (Å^{-3})	2400 K	0.0593	0.0587	0.0570	
	1400 K	0.0628	0.0632	0.0609	
CN	2400 K	13.4	13.0	12.4	
	1400 K	13.8	13.4	13.0	

[a]Averaged over peak.

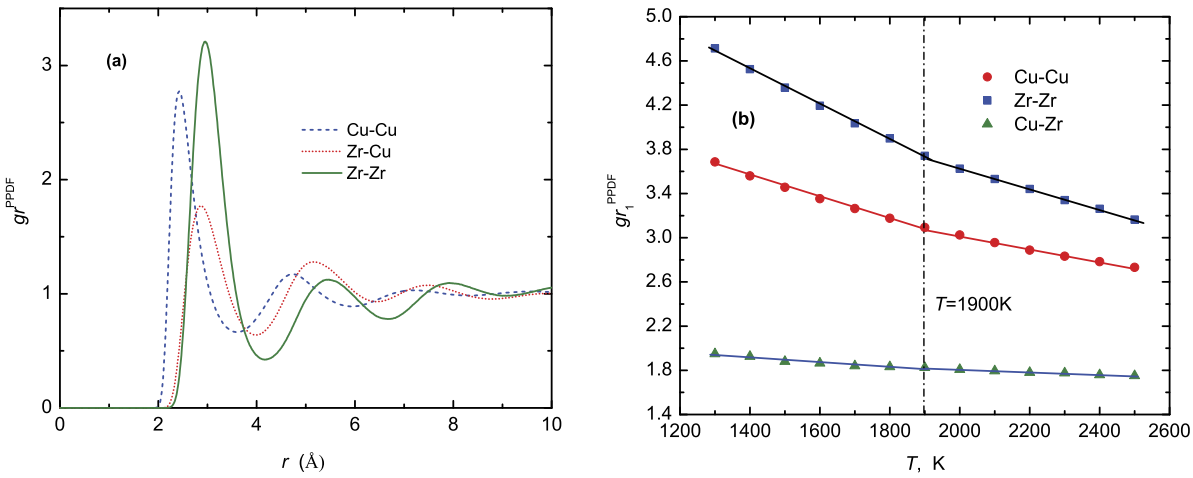

FIG. 7. Static partial pair distribution functions (PPDFs) of liquid Cu_8Zr_3 (a) PPDFs for Cu-Cu, Zr-Cu, and Zr-Zr pairs at 2400 K; (b) intensities of the first peaks of the PPDFs for the three pairs at different temperatures.

Taking their values and the ones of other evaluations of experiments,[59–61] one finds ranges for the peak positions of (2.48-2.63), (2.74-2.84), and (2.97-3.26) Å, for the Cu-Cu, Cu-Zr, and Zr-Zr pairs, respectively. Our values fall into those ranges. The values obtained from an *ab initio* calculation[62] again fall into these ranges.

The intensities of the first peaks, $g^{\mathrm{PPDF}}(r_1)$ are plotted against temperature in Fig. 7(b). Similar to the case of total PDF, there is also a kink in the temperature dependence of $g^{\mathrm{PPDF}}(r_1)$ for three pairs at a temperature close to T_s = 1900 K. The least pronounced kink is for the Cu-Zr pairs.

In Fig. 8, we present the normalized coordination numbers, $CN_s = CN_T/CN_0$, as function of temperature, where CN_T denotes the coordination number at a given temperature T, and CN_0 the coordination number at the highest temperature (T = 2400 K). CN_0 takes 8.7, 9.8, and 5.6 for Cu-Cu, Zr-Cu, and Zr-Zr pairs, respectively. A Cu-atom has an average of 12.4 neighbors, whereas a Zr-atom has 15.4 neighbors. The occupancy of the first shell by the two atomic species varies slightly with temperature. A kink in the temperature

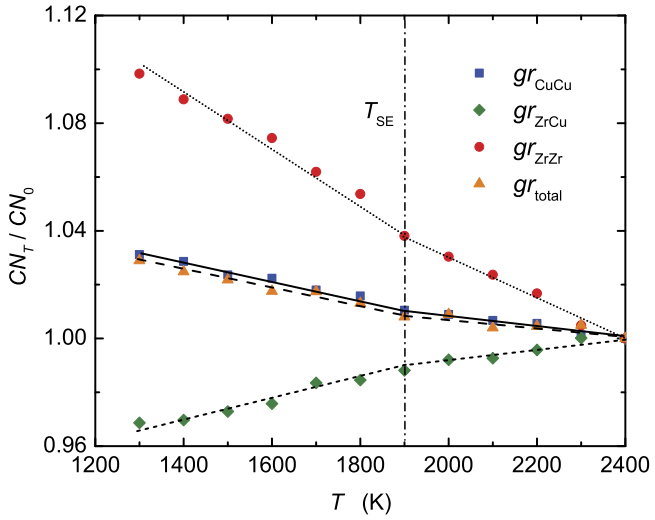

FIG. 8. Normalized partial and total coordination numbers in liquid Cu_8Zr_3 versus temperature.

dependence of CN_s is clearly seen at 1900 K for all three pairs. This means that at temperatures below 1900 K, $CN_T^{\mathrm{Cu-Cu}}$ and $CN_T^{\mathrm{Zr-Zr}}$ increase, whereas $CN_T^{\mathrm{Zr-Cu}}$ decreases more rapidly with the decrease of the temperature. Therefore, one atom has a stronger affinity to another atom of the same type, namely, one atom prefers to the site around another atom of the same type. The change of reduced CN with temperature for the total PDF is also given in Fig. 8, and CN_0 is around 13.4 at 2400 K. Similar to Cu-Cu, Zr-Cu, and Zr-Zr pairs, there is also a kink in the temperature dependence of CN for the total PDF at around 1900 K.

2. Time dependent pair distribution function

From Eq. (10), we calculate the time dependent partial pair distribution functions of liquid Cu_8Zr_3 at different temperatures, shown in Fig. 9 for T = 1800 K. The time dependent PPDF for Cu-Cu, $g(r,t)_{\mathrm{Cu-Cu}}$, shows for t = 0 a self-hole stretching to about r = 2.0 Å in radius. With time, the height of the first and second peaks decreases, indicating the loss of short range order. At around 1.0 ps, the second peak disappears, and after about 3.5 ps also the first peak vanishes. Simultaneously the self-hole is gradually filled by Cu atoms. When t exceeds about 3.0 ps, $g(r,t)_{\mathrm{Cu-Cu}}$ in the region of the self-hole exceeds the average value of 1.0. For example, $g(r,t)_{\mathrm{Cu-Cu}} \approx 1.05$ for $r \in (0.0, 2.44$ Å) when t = 3.5 ps. This indicates that there is an overshooting of the hole-filling, and the number of Cu atoms filling to the hole left by a Cu atom exceeds the statistical average value. The overshooting of the hole-filling becomes most pronounced at around 8.0 ps, where the height of the peak reaches 1.16 at r = 0. Then the overshooting of hole-filling weakens with the further evolution of the system, and it finally vanishes completely, as is seen in the case of t = 50.0 ps. This means that for Cu at 1800 K, the system will go back to the viscous flow with time. This overshooting was previously reported for $CuZr_2$[42] where the effect is even more pronounced.

The time evolution of the PPDF for Zr-Zr, $g(r,t)_{\mathrm{Zr-Zr}}$, resembles the one of $g(r,t)_{\mathrm{Cu-Cu}}$, Fig. 9(b). Again there is an overshooting of hole-filling for Zr-Zr, indicating that a

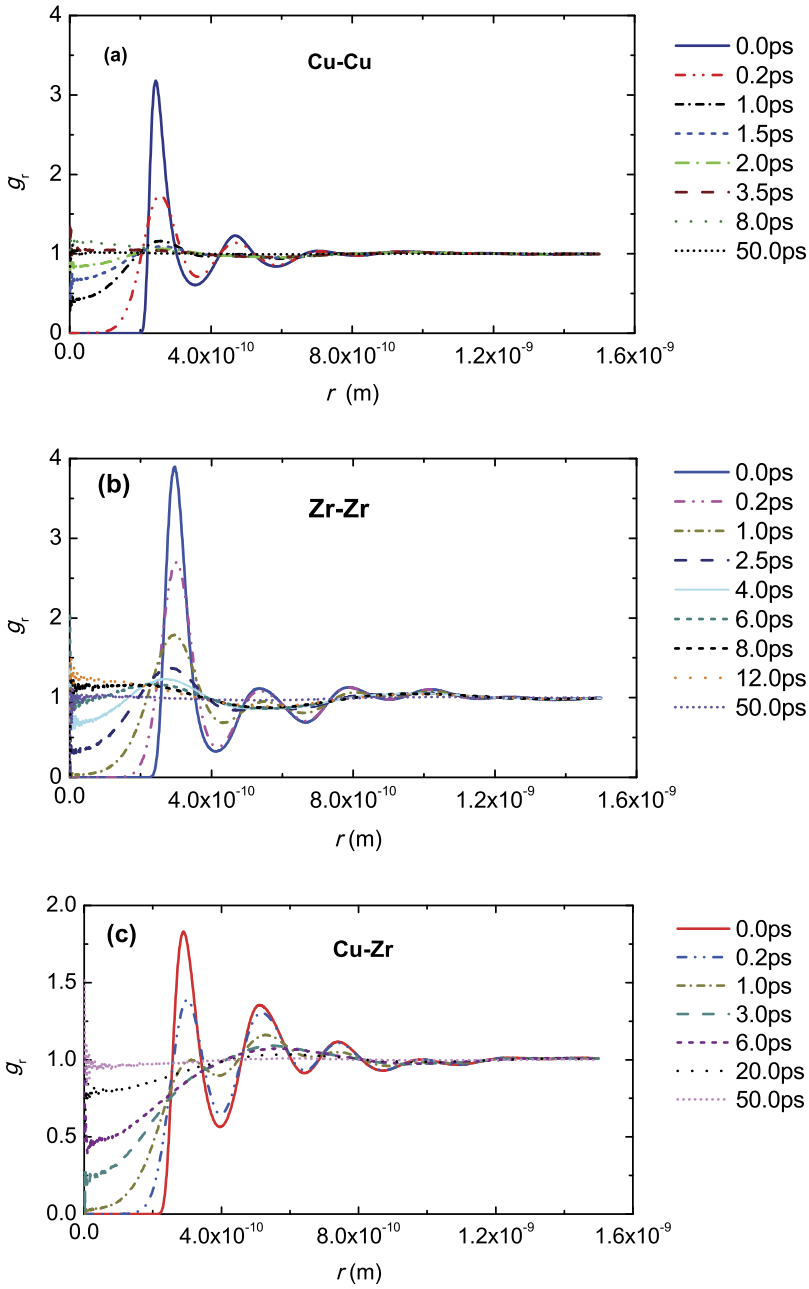

FIG. 9. Time dependent PPDFs for Cu-Cu, Cu-Zr, and Zr-Zr pairs in liquid Cu_8Zr_3 at 1800 K.

previous Zr site is preferentially filled by another Zr atom before the system goes back to the viscous flow. On the other hand, no overshooting is visible in the PDF of Cu-Zr, Fig. 9(c). We can see that the self-hole of Cu is gradually filled by Zr atoms, as expected by the viscous flow.

3. Relative occupation number of self-hole

To study the decay of the partial pair-correlation in more detail, following Refs. 42 and 63, we define a time and temperature dependent relative number of atoms in a spherical shell

$$n_{\alpha\beta}(T,t) = \frac{1}{V_{12}} \int_{r_1}^{r_2} g_{\alpha\beta}(r,t) 4\pi r^2 dr, \qquad (16)$$

where V_{12} is the volume of the shell from r_1 to r_2. $n_{\alpha\beta}(T,t)$ measures the number of atoms of species β in the volume V_{12}, normalized to their random ($t = \infty$) value, under the condition that at time $t = 0$ a different atom (species α) was at $r = 0$. By definition $n_{\alpha\beta}(T, t = \infty) = 1$.

With a common radius of the self-hole, $r_1 = 0$ and $r_2 = 1.9$ Å, we calculate the relative occupation number of the self-hole at different temperatures, Fig. 10. As we see from Fig. 10(a), there is, for all temperatures, an overshooting of $n_{\mathrm{CuCu}}(T,t)$ above the random value of 1.0 in the ps time scale, similar to but less pronounced than observed for Cu in liquid $CuZr_2$. It indicates a preference of Cu to occupy former Cu sites. In liquid $CuZr_2$, $n_{\mathrm{ZrZr}}(T,t)$ developed monotonously in time following a simple exponential function of time t, which is expected from normal diffusion with no fixed jump length. In the contrast, as seen from Fig. 10(b), in Cu_8Zr_3 there is also an overshooting of $n_{\mathrm{ZrZr}}(T,t)$ above the long time limit of 1.0, even slightly enhanced compared to that of $n_{\mathrm{CuCu}}(T,t)$. This means that the self-hole of Zr atom is first filled by another

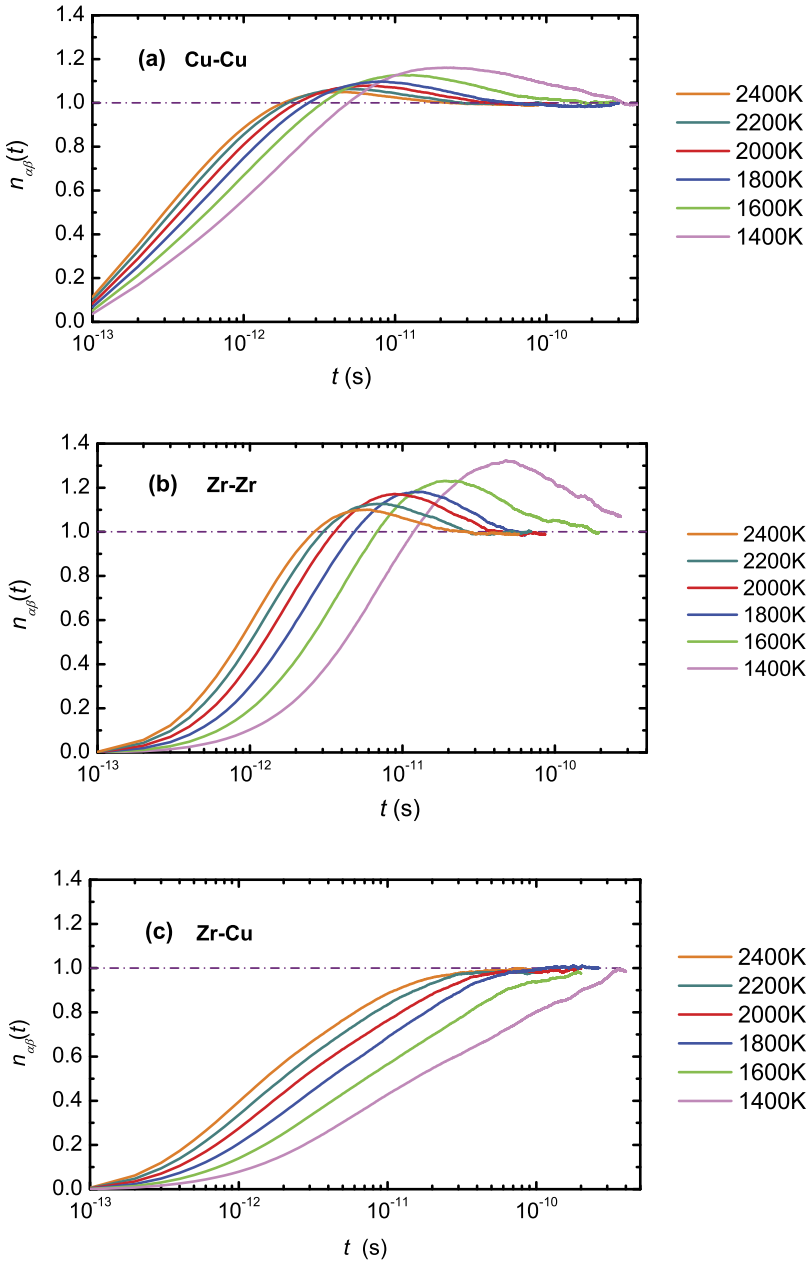

FIG. 10. Time dependent relative occupation numbers of the self-holes for the three pairs in liquid Cu_8Zr_3 at temperatures from 1400 K to 2400 K (right to left).

Zr atom with a large probability, and then the probability drops to the statistical average of 1.0. From Fig. 10(c), we can see that the filling of the self-hole left by Cu atoms with the approximate concentration of Zr atoms, $n_{\mathrm{CuZr}}(T,t)$, is monotonous and a simple exponential form of time expected from normal diffusion, as is similar to the case of Zr-Zr and Cu-Zr in $CuZr_2$.

Both the time dependent pair distribution function and the relative occupation number of self-hole indicate that the difference in the dynamics of the self-hole filling between two components in liquid Cu_8Zr_3 is not as pronounced as in liquid $CuZr_2$. This explains why the temperature T_s where the SE relation breaks down in liquid Cu_8Zr_3 is the same for both components, whereas in liquid $CuZr_2$ there is a temperature difference of 300 K for the breakdown of SE relation.

If we define the hole-filling time $\tau(T)$ using a value of $n_{\alpha\beta}(T,t)$, for example, $n_{\alpha\beta}(T,t) = 0.8$, we can derive the temperature dependence of $\tau(T)$, from which we could discuss the change of dynamics of the liquid during its cooling down. In Fig. 11, in a semi-logarithmic scale, $\tau(T)$ at different temperatures are illustrated. A kink at 1900 K can be seen in the three τ-T curves. Both in the HT and LT regimes of the self-hole filling time, separated by this kink, τ can be expressed as

$$\tau(T) = \tau_0 \exp\left(\frac{Q}{RT}\right), \tag{17}$$

where τ_0 is a prefactor of self-hole filling time, R is the gas constant, and Q is the activation energy for self-hole filling. Fitting parameters for three pairs are as follows: $\tau_{\text{Cu-Cu,HT}} = 0.186$ ps, $Q_{\text{Cu-Cu,HT}} = 27\,325$ J/mol; $\tau_{\text{Cu-Cu,LT}} = 0.111$ ps, $Q_{\text{Cu-Cu,LT}} = 35\,328$ J/mol; $\tau_{\text{Cu-Zr,HT}} = 0.202$ ps, $Q_{\text{Cu-Zr,HT}} = 67\,790$ J/mol; $\tau_{\text{Cu-Zr,LT}} = 0.065$ ps, $Q_{\text{Cu-Zr,LT}} = 84\,812$ J/mol; $\tau_{\text{Zr-Zr,HT}} = 0.243$ ps, $Q_{\text{Zr-Zr,HT}} = 37\,244$ J/mol; and $\tau_{\text{Zr-Zr,LT}} = 0.108$ ps, $Q_{\text{Zr-Zr,LT}} = 49\,917$ J/mol. In comparison with other Qs in this work, we find that the activation energy

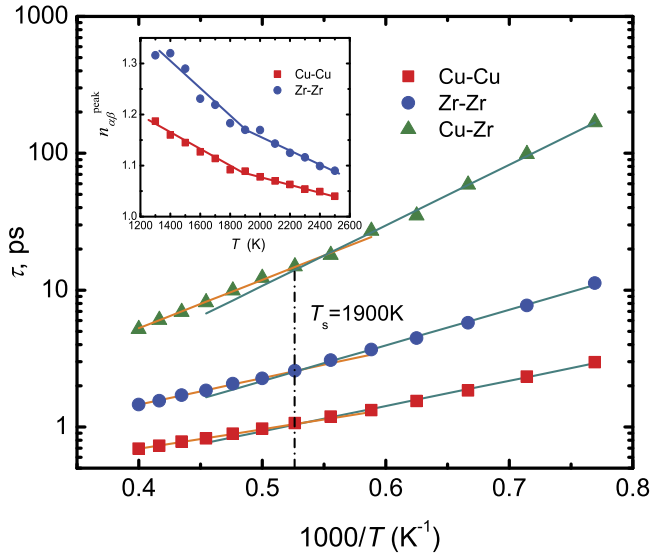

FIG. 11. Self-hole filling time defined by $n(\tau) = 0.8$ for three pairs in liquid Cu_8Zr_3. The inset demonstrates the change of the intensity of the relative number of self-hole filling with the temperature.

for self-hole filling of Zr-Zr at temperatures above T_s, $Q_{Zr\text{-}Zr,HT}$ = 37 244 J/mol, is quite close to the Q-value derived from viscosity, Q_{eta} = 38 030 J/mol. The kink in the self-hole filling time can be more clearly seen in a plot of the peak value of the self-hole filling, $n_{\alpha\beta}^{peak}$, as shown in the inset. Apparently, τ changesfaster at temperatures below 1900 K, which means that the filling of the self-holes takes longer time than expected from the variation at high temperatures above 1900 K. The dynamics of the liquid slows down at 1900 K or becomes heterogeneous.

4. Dynamic heterogeneity

In order to elucidate the dynamic heterogeneity and its correlation with the self-hole filling, we calculate the non-Gaussianity parameter $\alpha_2(t)$,

$$\alpha_2(t) = \frac{3\langle \Delta r^4(t) \rangle}{5\langle \Delta r^2(t) \rangle^2} - 1, \tag{18}$$

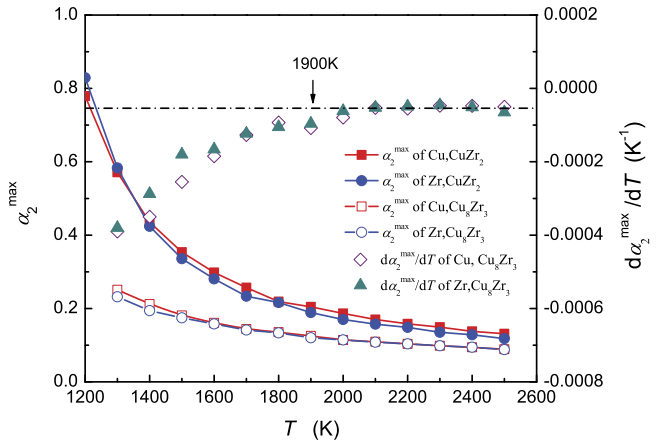

FIG. 12. Maximum of the non-Gaussianity parameter α_2^{max} and its temperature derivative for the two species in liquid Cu_8Zr_3 against temperature. The α_2^{max} of liquid $CuZr_2$ is included for comparison.

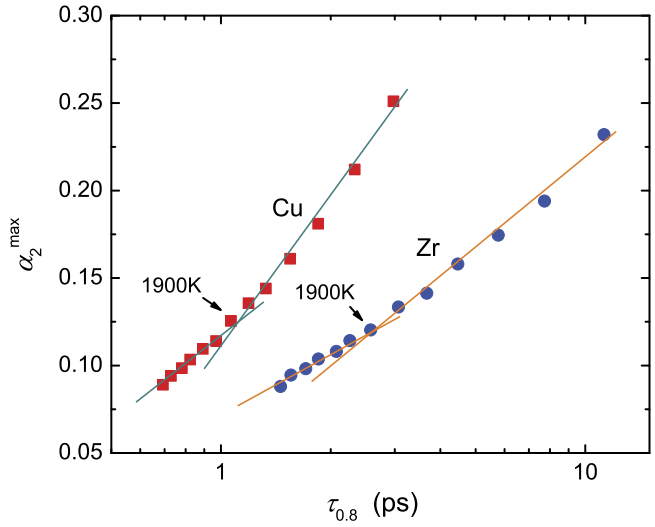

FIG. 13. Change of α_2^{max} with the self-hole filling time defined by $n(\tau) = 0.8$.

where $\Delta r^2(t)$ and $\Delta r^4(t)$ are the mean square and quartic displacements, and $\langle \ldots \rangle$ denotes the average over all atoms of one species and over the starting times t_0. The behavior of $\alpha_2(t)$ for Cu and Zr in liquid Cu_8Zr_3 is similar to the one observed in other liquids.[64–66] For brevity, in Fig. 12, we only show the maximal non-Gaussianity parameter, α_2^{max}, and its temperature derivative, d(α_2^{max})/dT, for liquid Cu_8Zr_3 and $CuZr_2$. The dynamic heterogeneity of liquid Cu_8Zr_3 is much lower than that of liquid $CuZr_2$. For example, at 1400 K for Zr, α_2^{max} in liquid $CuZr_2$ is 0.424, whereas it is only 0.194 in liquid Cu_8Zr_3. The variation of d(α_2^{max})/dT with temperature demonstrates that the rate of increase of the dynamic heterogeneity of liquid Cu_8Zr_3 increases rapidly below 1900 K. This temperature is again close to the breakdown temperature of the SE relation.

To elucidate the connection between self-hole filling and dynamic heterogeneity, we show in Fig. 13, the maximum of the non-Gaussianity, $\alpha_2^{max}(T)$, against the self-hole filling time τ (T) in a semi-logarithmic plot. The hole filling time increases exponentially with $\alpha_2^{max}(T)$, τ (T) ~exp($c\alpha_2^{max}(T)$). The constant c changes at T = 1900 K, when the temperature derivative of $\alpha_2^{max}(T)$ changes, see Fig. 12.

IV. DISCUSSION

In this work, we found a strong correlation among transport properties, microscopic dynamics of atomic motion, and structure. Such correlations have also been reported for a number of materials, e.g., Lennard-Jones and soft sphere systems.[66] When the temperature drops to the onset of the breakdown of the SE relation, T_{SE}, the viscosity begins to deviate from the high temperature Arrhenius behavior. Meanwhile, the first derivative of the ratio of the two diffusion coefficients, d/dT(D_{Cu}/D_{Zr}), changes significantly, indicating that the two components are affected differently by the change in dynamics. The product of D_{Zr} and η starts to exhibit a MCT-like behavior, namely, $D_{Zr}\cdot\eta \approx const$. The variation of these two parameters and the MCT-like law hint to a change

in the nature of the atomic motion at T_{SE}, and this is further confirmed by a change of the non-Gaussianity of motion and by detailed analysis of the self-hole filling dynamics of the two components. We found a pronounced kink in the variation of the self-hole filling time with temperature. At temperatures below T_{SE}, although the change of the self-hole filling time still obeys an Arrhenius law, the activation energy increases by up to 40%. This means that the self-hole filling dynamics slows down or becomes heterogeneous below T_{SE}. The breakdown of the SE relation at T_{SE} is also accompanied by a change of the local structure. The analysis of the static partial distribution function demonstrates that there is a kink in the temperature dependence of the intensity of the first peak. As a result, the partial coordination numbers of Cu-Cu and Zr-Zr increase more rapidly at temperatures below T_{SE}. This change of the localized structure increases the probability of preferential replacement of self-holes of the two components by atoms of the same type, which contributes to D_{Cu} and D_{Zr}. This alleviates the influence of self-hole filling speed's decrease on the diffusion coefficient. On the other hand, the viscosity increases due to the slowing down of the self-hole filling dynamics. As a result, both $D_{Cu}\cdot\eta$ and $D_{Zr}\cdot\eta$ become larger than expected from the SE relation, i.e., the SE relation has broken down.

In our previous work of liquid $CuZr_2$, the marked change of $d/dT(D_{Cu}/D_{Zr})$ is ascribed to the rapid increase of dynamical heterogeneity,[10] which is further related to the collectivity of the jump process in undercooled liquids and glasses in our earlier work.[64] Therefore, the change in the nature of atomic motion at T_{SE} is assumed to be the crossover from a normal viscous flow to the one which can be dissected into separate jumps.[46] Different from the low temperature glass, the time between such jumps is too short for thermalisation between them. In an energy landscape description,[67–69] the underlying structure of the landscape becomes important but the system is not yet caught in a basin for sufficient times to thermalize. At temperatures above T_{SE}, the flow in the melt is dominated by binary collisions, whereas when the temperature decreases below T_{SE}, collective motion of atoms is more effective, string-like structures appear in diffusion, and local structures decay more slowly. In the previously studied $CuZr_2$ melt, particularly the matrix of Zr atoms is rather sluggish compared to the Cu atoms. A Cu atom would, therefore, sit more comfortably on a site vacated by another Cu atom. In addition, the decay of the enhanced site occupation is slowed down by Cu-Cu correlations.[37] The difference between Cu and Zr in their local dynamics is not so much due to differences in the jump vectors but due to enhanced residence times. The jumps are collective involving many atoms and no preferred jump length was observed. A similar effect was observed in a binary Lennard-Jones system.[70] In the present system, no such globally sluggish Zr matrix exists. The overshoots in hole-filling appear for both Zr and Cu. It is somewhat enhanced for the minority (Zr) species but much less than for Zr in $CuZr_2$. Looking at the average self-hole filling, we get similar numbers for both compositions. We ascribe this effect to the rise in heterogeneity with decreasing temperature. At any given time, some atoms participate in diffusive modes whereas others remain sluggish and thus again form a quasi-matrix for the fast atoms. The effect is enhanced by the string- (chain-) like structure of motion. Such motion does not necessarily cause large disturbances of neighborhoods, as evidenced by the observed low activation volumes.[77] We, therefore, conclude that the hole-filling dynamics of the different components is not only controlled by atomic mobility but also by size and chemical mismatch. In $CuZr_2$, the size of a Zr atom is close to the average whereas in Cu_8Zr_3 it is seriously too big. The average matrix is expanded around a Zr atom which again favors occupancy of a previously occupied site. This mechanism is most efficient when the mobility centers are spread out over the system as opposed to be concentrated in regions of lower density.

We related the breakdown of the SE relation to changes of both structure and dynamic heterogeneity. The connection between these is quite subtle. In glasses, one can relate the stability of local structures with soft quasi-local vibrations.[71] If one defines some value characterizing the quality of the structure, analogous to the potential energy, the matrix of second derivatives with respect to atomic position is strongly correlated with the dynamical matrix of the vibrations. Direct correlations between structure and vibrations are not so clear. In particular, soft quasi-local vibrations are found from both the structural and energetic dynamic matrixes. Soft quasi-local vibrations correlate with local high mobility.[72] In a similar approach, local atomic stresses are correlated with vibrations and mobility.[73] This means that high mobility is related to small structural changes, as seen by second derivatives. Although we have seen correlations of both structural changes and dynamic heterogeneity with the SE breakdown, we cannot give a quantitative relation between them.

An alternative explanation would be by a temporary trapping of atoms. Correlations between local structure and mobility are also reported for the liquid state where it was observed that atoms participating in some clusters, e.g., icosahedra are less mobile than others.[74] These structural influences provide a connection between structural and dynamic heterogeneity. To explain the differences in the self-hole filling dynamics, a strong concentration dependence would be needed, which, however, has not been observed.[59–61] An alternative would be that the difference is not due to slow structures but due to the concentration dependence of the highly mobile structures. Even though we cannot fully exclude such a scenario, it is hard to imagine such an atomic scenario compatible with the known information.

Dynamics is the key factor for the breakdown of the SE relation, so the difference in dynamics of the two components determines whether SE relation for each component breaks down at similar temperatures. In liquid $CuZr_2$, the dynamics of the two components is quite different. This leads to a difference between T_{SE} for Cu and that for Zr of about 300 K. In contrast, in liquid Cu_8Zr_3, the sites of the two components are both preferably filled by another atom of their own type before the filling probability drops to the statistical average. The similarity of the dynamics of atomic motion of the two components in liquid Cu_8Zr_3 explains why the SE relation for both Cu and Zr breaks down at a similar temperature.

We have already verified the validity of $d(D_1/D_2)/dT$ in predicting the onset temperature of the abnormal breakdown of SE relation at temperatures far above T_c in liquids of Lennard-Jones,[53] $CuZr_2$,[10] and Cu_8Zr_3. Noticeably, these systems are particular in which the bonding between the two components is weak.[46] We need further work to elucidate whether these criteria can be used to describe the abnormal breakdown of SE relation in a strong bonding system, such as Ni-Zr,[75–77] Ni-Zr-Al,[9] and a binary Lennard-Jones system,[78] whose self-diffusion coefficients in the melt run nearly parallel to each other with the temperature. On the other hand, $d(D_1/D_2)/dT$ is confined to a multi-component system, and it cannot be applied to monatomic systems, whose T_{SE} might be predicted by the deviation of viscosity from the Arrhenius behavior of high temperatures.

We distinguish the strong breakdown of SE relation near T_c in other studies[24–29] and the change of law of the SE relation at T_{SE}, far above T_c, in this work. The former is in a temperature region where isolated hopping events, with thermalization in between, are observed as opposed to the "hopping" producing flow discussed here. We are looking at a temperature regime where the heterogeneity is still moderate. Some effects seen at lower temperatures might not be observable in the present regime. How far this MCT-like regime extends will be material dependent. It is, however, observed experimentally.[32]

V. CONCLUSIONS

Using a modified EAM potential, we calculated by MD the viscosity and self-diffusion coefficients of a Cu_8Zr_3 melt at temperatures from 1300 to 2400 K. The shear viscosity is calculated from Green-Kubo equation and the diffusion coefficient evaluated from the long time limits of the mean-square displacements. The critical temperature of mode coupling theory T_c is derived as 930 K from the variations of the two diffusivities and viscosity. The Stokes-Einstein relation is violated below $T_{SE} = 1900$ K, which is around 1000 K above T_c. At temperatures below T_{SE}, the product of D and η fluctuates around a constant value, which is in striking contrast to the SE relation but according to the prediction of MCT about diffusion and viscosity near T_c.

The abnormal breakdown of SE relation correlates with the changes of liquid structure and the temperature dependences of three parameters, i.e., D_{Cu}/D_{Zr}, η, and self-hole filling time. The more rapid increase of the partial coordination numbers for Cu-Cu and Zr-Zr pairs indicates a larger affinity between atoms of the same type and a more pronounced short range order when the liquid is cooled below T_{SE}. The rapid change of $d(D_1/D_2)/dT$ at T_{SE} means a rapid increase of dynamical heterogeneity due to the collective motion of atoms. The kink in the temperature dependence of self-hole filling time and the increase of activation energy of 40% hints to a slowing down of self-hole filling dynamics.

The analysis of self-hole filling indicates that the self-hole left by one atom after it moves away from its original site is preferentially filled by another atom of the same type. Due to the similar preferential self-hole filling dynamics, the SE relation in liquid Cu_8Zr_3 breaks down at similar temperatures for the two components, in contrast to the case of liquid $CuZr_2$. The more pronounced short range order and the preferential self-hole filling for atoms of the same type contribute to the two self-diffusion coefficients and alleviate the influence of the slowing down of the hole filling dynamics, which contributes to the viscosity. The breakdown of SE relation is the joint effects of the change of structure and dynamics.

The parameter $d(D_1/D_2)/dT$ suggested previously was further validated in this work to predict quantitatively the onset of the abnormal breakdown of SE relation. We here further propose that the deviation of viscosity from its high temperature Arrhenius behavior can also be used to predict T_{SE}. This facilitates the quantitative prediction of T_{SE} in the absence of diffusion data.

ACKNOWLEDGMENTS

Financial support from the National Natural Science Foundation of China (Grant No. 51171115), National Basic Research Program of China under Contract No. 2011CB012900, Program for New Century Excellent Talents in University, Shanghai Municipal Natural Science Foundation (Grant No. 10ZR1415700), and Research Fund for the Doctoral program of Higher Education of China (Grant No. 20100073120008) are acknowledged. This work is partially supported by Alexander-von-Humboldt Foundation.

APPENDIX: INFLUENCE OF THE DEFINITION OF SELF-HOLE FILLING TIME

In order to elucidate the influence of the definition of hole-filling time, we illustrate the self-hole filling time, $\tau_{ZrZr}(T)$, in Fig. 14 for two different cutoffs of $n_{\alpha\beta}(T,t)$, i.e., 0.8 and 0.9. Clearly, the hole-filling time for the two definitions runs almost parallel to each other. When we use $n_{\alpha\beta}(T,t) = 0.8$ to define hole-filling time, $\tau_{0,HT} = 0.24$ ps, and $Q_{HT} = 37\,245$ J/mol, $\tau_{0,LT} = 0.11$ ps, and $Q_{LT} = 49\,916$ J/mol. And when we

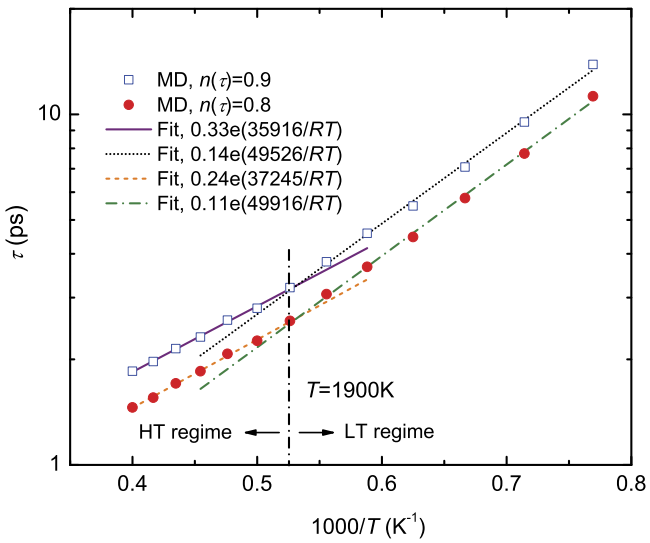

FIG. 14. Comparison of the temperature dependence of self-hole filling time defined by different methods.

use $n_{\alpha\beta}(T,t) = 0.9$, $\tau_{0,\mathrm{HT}} = 0.33$ ps, $Q_{\mathrm{HT}} = 35\,916$ J/mol, $\tau_{0,\mathrm{LT}} = 0.14$ ps, and $Q_{\mathrm{LT}} = 49\,526$ J/mol. Moreover, in both cases, there is a kink in the τ-T curve at around 1900 K. This means that different definitions of self-hole filling time lead to the same conclusion that the dynamics slows down or becomes heterogeneous at 1900 K.

[1]A. Einstein, Ann. Phys. **322**, 549 (1905).
[2]L. D. Landau and E. M. Lifshitz, Fluid Mechanics (Pergamon Press, Oxford, 1959).
[3]H. J. V. Tyrrell and K. R. Harris, *Diffusion in Liquids* (Butterworths, London, 1984).
[4]U. Balucani and M. Zoppi, *Dynamics of the Liquid State* (Clarendon, Oxford, 1994).
[5]M. G. McPhie, P. J. Daivis, and I. K. Snook, Phys. Rev. E **74**, 031201 (2006).
[6]S. Bhattacharyya and B. Bagchi, J. Chem. Phys. **106**, 1757 (1997).
[7]F. Ould-Kaddour and D. Levesque, Phys. Rev. E **63**, 011205 (2001).
[8]J. R. Schmidt and J. L. Skinner, J. Chem. Phys. **119**, 8062 (2003).
[9]M. Guerdane, Ph.D. thesis, University Goettingen, Germany, 2000.
[10]X. J. Han and H. Schober, Phys. Rev. B **83**, 224201 (2011).
[11]T. Kawasaki and A. Onuki, Phys. Rev. E **87**, 012312 (2013).
[12]S. Sengupta and S. Karmakar, J. Chem. Phys. **140**, 224505 (2014).
[13]P. Kumar, S. V. Buldyrev, S. R. Becker, P. H. Poole, F. W. Starr, and H. E. Stanley, Proc. Natl. Acad. Sci. U. S. A. **104**, 9575 (2007).
[14]A. Ikeda and K. Miyazaki, Phys. Rev. Lett. **106**, 015701 (2011).
[15]A. Noda, K. Hayamizu, and M. Watanabe, J. Phys. Chem. B **105**, 4603 (2001).
[16]S. F. Swallen, P. A. Bonvallet, R. J. McMahon, and M. D. Ediger, Phys. Rev. Lett. **90**, 015901 (2003).
[17]M. K. Mapes, S. F. Swallen, and M. D. Ediger, J. Phys. Chem. B **110**, 507 (2006).
[18]M. D. Ediger, P. Harrowell, and L. Yu, J. Chem. Phys. **128**, 034709 (2008).
[19]K. L. Ngai, J. H. Magill, and D. J. Plazek, J. Chem. Phys. **112**, 1887 (2000).
[20]T. Wu and L. Yu, J. Phys. Chem. B **110**, 15694 (2006).
[21]A. C. Pan, J. P. Garrahan, and D. Chandler, Phys. Rev. E **72**, 041106 (2005).
[22]P. G. Debenedetti and F. H. Stillinger, Nature **410**, 259 (2001).
[23]Z. Shi, P. G. Debenedetti, and F. H. Stillinger, J. Chem. Phys. **138**, 12A526 (2013).
[24]V. Zöllmer, K. Rätzke, and F. Faupel, J. Mater. Res. **18**, 2688 (2003).
[25]V. Zöllmer, K. Rätzke, F. Faupel, and A. Meyer, Phys. Rev. Lett. **90**, 195502 (2003).
[26]D. Thirumalai and R. D. Mountain, Phys. Rev. E **47**, 479 (1993).
[27]I. Chang and H. Sillescu, J. Phys. Chem. B **101**, 8794 (1997).
[28]E. Rössler, Phys. Rev. Lett. **65**, 1595 (1990).
[29]A. Meyer, Phys. Rev. B **66**, 134205 (2002).
[30]W. Goetze and L. Sjogren, Rep. Prog. Phys. **55**, 241 (1992).
[31]A. Meyer, W. Petry, M. Koza, and M. P. Macht, Appl. Phys. Lett. **83**, 3894 (2003).
[32]J. Brillo, A. I. Pommrich, and A. Meyer, Phys. Rev. Lett. **107**, 165902 (2011).
[33]A. Jaiswal, T. Egami, and Y. Zhang, Phys. Rev. B **91**, 134204 (2015).
[34]H. R. Schober, Physics **4**, 80 (2011).
[35]H. Sillescu, J. Non-Cryst. Solids **243**, 81 (1999).
[36]R. Yamamoto and A. Onuki, Phys. Rev. Lett. **81**, 4915 (1998).
[37]S. R. Becker, P. H. Poole, and F. W. Starr, Phys. Rev. Lett. **97**, 055901 (2006).
[38]M. D. Ediger, Annu. Rev. Phys. Chem. **51**, 99 (2000).
[39]S. C. Glotzer, J. Non-Cryst. Solids **274**, 342 (2000).
[40]L. Ngai, J. Phys. Chem. B **103**, 10684 (1999).
[41]L. Ngai, Philos. Mag. **87**, 357 (2007).
[42]M. Kluge and H. R. Schober, J. Non-Cryst. Solids **352**, 5093 (2006).
[43]M. Parrinello and A. Rahman, Phys. Rev. Lett. **45**, 1196 (1980).
[44]W. G. Hoover, Phys. Rev. A **31**, 1695 (1985).
[45]M. I. Baskes and R. A. Johnson, Modell. Simul. Mater. Sci. Eng. **2**, 147 (1994).
[46]M. Kluge and H. R. Schober, Phys. Rev. B **70**, 224209 (2004).
[47]C. Gaukel, *Dynamics of Glasses and Undercooled Melts of Zr-Cu*, Berichte des Forschungszentrums Jülich Vol. 3556 (Forschungszentrum Jülich, Jülich, Germany, 1998).
[48]M. P. Allen and D. J. Tildesley, *Computer Simulation of Liquids* (Clarendon Press, Oxford, 1987).
[49]C. Rapaport, *The Art of Molecular Dynamics Simulation* (Cambridge University Press, Cambridge, 1995).
[50]F. Yang, D. Holland-Moritz, J. Gegner, P. Heintzmann, F. Kargl, C. C. Yuan, G. G. Simeoni, and A. Meyer, Europhys. Lett. **107**, 46001 (2014).
[51]M. I. Mendelev, M. J. Kramer, R. T. Ott, D. J. Sordelet, D. Yagodin, and P. Popel, Philos. Mag. **89**, 967 (2009).
[52]M. I. Mendelev, D. J. Sordelet, and M. J. Kramer, J. Appl. Phys. **102**, 043501 (2007).
[53]P. Bordat, F. Affouard, M. Descamps, and F. Müller-Plathe, J. Phys.: Condens. Matter **15**, 5397 (2003).
[54]Y. J. Lü, H. Cheng, and M. Chen, J. Chem. Phys. **136**, 214505 (2012).
[55]S. Plimpton, J. Comput. Phys. **117**, 1 (1995), See http://lammps.sandia.gov for information about LAMMPS Molecular Dynamics Simulator.
[56]Y. Q. Cheng, E. Ma, and H. W. Sheng, Phys. Rev. Lett. **102**, 245501 (2009).
[57]V. Wessels *et al.*, Phys. Rev. B **83**, 094116 (2011).
[58]M. E. Blodgett and K. F. Kelton, J. Non-Cryst. Solids **412**, 66 (2015).
[59]N. Mattern, A. Schöps, U. Kühn, J. Acker, O. Khvostikova, and J. Eckert, J. Non-Cryst. Solids **354**, 1054 (2008).
[60]N. Mattern, P. Jovari, I. Kaban, S. Gruner, A. Elsner, V. Kokotin, H. Franz, B. Beuneu, and J. Eckert, J. Non-Cryst. Solids **485**, 163 (2009).
[61]D. Ma, A. D. Stoica, X.-L. Wang, Z. P. Lu, M. Xu, and M. Kramer, Phys. Rev. B **80**, 014202 (2009).
[62]N. Jakse and A. Pasturel, Phys. Rev. B **78**, 214204 (2008).
[63]M. Kluge, *Molecular dynamics simulations of the diffusion in binary $Cu_{33}Zr_{67}$ metallic melt and glass*, Berichte des Forschungszentrums Jülich Vol. 3913 (Forschungszentrum Jülich, Jülich, Germany, 2001).
[64]D. Caprion, J. Matsui, and H. R. Schober, Phys. Rev. Lett. **85**, 4293 (2000).
[65]W. Kob, C. Donati, S. J. Plimpton, P. H. Poole, and S. C. Glotzer, Phys. Rev. Lett. **79**, 2827 (1997).
[66]S. Sengupta, S. Karmakar, C. Dasgupta, and S. Sastry, J. Chem. Phys. **138**, 12A548 (2013).
[67]M. Goldstein, J. Chem. Phys. **51**, 3728 (1969).
[68]H. Stillinger, Science **267**, 1935 (1995).
[69]S. Sastry, P. G. Debenedetti, and F. H. Stillinger, Nature **393**, 554 (1998).
[70]T. B. Schroeder, Ph.D. thesis, Roskilde University, Roskilde, Denmark, 2000; e-print arXiv:cond-mat/0005127.
[71]V. A. Luchnikov, N. N. Medvedev, Yu. I. Naberukhin, and H. R. Schober, Phys. Rev. B **62**, 3181 (2000).
[72]C. Oligschleger and H. R. Schober, Phys. Rev. B **59**, 811 (1999).
[73]V. A. Levashov, T. Egami, R. S. Aga, and J. R. Morris, Phys. Rev. B **78**, 064205 (2008).
[74]Y. Zhang, C. Z. Wang, F. Zhang, M. I. Mendelev, M. J. Kramer, and K. M. Ho, Appl. Phys. Lett. **105**, 151910 (2014).
[75]H. Teichler, Phys. Rev. Lett. **76**, 62 (1996).
[76]H. Teichler, J. Non-Cryst. Solids **293-295**, 339 (2001).
[77]F. Faupel *et al.*, Rev. Mod. Phys. **75**, 237 (2003).
[78]H. R. Schober, Phys. Rev. Lett. **88**, 145901 (2002).